



The impact of vegetation and soil parameters in simulations of surface energy and water balance in the semi-arid sahel: A case study using SEBEX and HAPEX-Sahel data

Daniel S. Kahan^a, Yongkang Xue^{a,b,*}, Simon J. Allen^c

^a*Department of Geography, University of California, Los Angeles, USA*

^b*Department of Atmospheric and Oceanic Sciences, University of California, Los Angeles, USA*

^c*CECS, University of Edinburgh, Edinburgh, UK*

Abstract

A series of numerical experiments has been designed to understand the physics at the land surface–atmosphere interface in the Sahel and to find the major parameters and parameterizations that are crucial to simulate arid climate processes. Observational data sets from the Sahelian Energy Balance Experiment (SEBEX) and the Hydrological Atmospheric Pilot Experiment (HAPEX-Sahel) were used to help interpret the results. The observational errors in these two data sets are examined first. In the control simulations, the standard type-8 (shrubs with ground-cover) data typically used by general circulation models for vegetation in the Sahel produce more than 50% underestimation of average latent heat flux and 100% overestimation of average sensible heat flux. The diurnal cycle of surface temperature may be overestimated during the day and underestimated at night. Sensitivity experiments were conducted to identify the most important parameters that affect Sahel simulation and their role at the surface/atmosphere interface. It was found that proper parameter estimation of leaf area index, stomatal resistance, and hydraulic conductivity allow enough evaporation to occur in land surface simulations. Sensible heat flux is thus reduced by greater partitioning of energy to latent heat flux. Proper parameter estimation of thermal diffusivity also impacts sensible heat flux and diurnal variation of surface temperature. In addition, the water balance may be misrepresented with standard parameter values by maintaining an unnecessarily high amount of soil moisture due to less evaporation. In general, the error existing between observations and simulation is reduced substantially by proper calibration of the vegetation/soil parameters.

© 2005 Elsevier Ltd. All rights reserved.

Keywords: Semi-arid area; Land parameters; Model validation

1. Introduction

Traditionally, the oceans were thought to be the only influence from the earth's surface worth

considering when studying climate change and weather patterns. However, starting with a study by Charney (1975), there have been many model simulations demonstrating that changes in the physical characteristics of the land surface may have a significant impact on climate. Land cover change can affect the climate by altering the partitioning of available energy between sensible and latent heat

* Corresponding author. Fax: +1 310 206 5976.

E-mail address: yxue@geog.ucla.edu (Y. Xue).

and by changing the partitioning of precipitation between evapotranspiration and runoff. Studies such as Dickinson and Henderson-Sellers (1988) and Xue and Shukla (1993) have shown that, through these effects, land cover change can cause changes in the atmosphere that feed back to the surface.

Although works such as these have increasingly demonstrated the importance of soils and vegetation in climate studies and substantial achievements have been made in parameterizing the physical and biological processes that occur at the land surface (e.g. Dickinson et al., 1986; Sellers et al., 1986; Bastidas et al., 1999), the variables used to describe the land surface have yet to be fully validated through scientific testing and comparison with observations. There is a considerable degree of uncertainty associated with the parameters derived using current procedures. The Model Parameter Estimation Experiment (MOPEX) is a continuing international project dedicated to developing techniques for the a priori estimation of parameters used in land surface parameterization schemes of atmospheric and hydrological models. MOPEX evolved to promote and guide the development of improved a priori parameter estimates (Duan et al., this issue; Hogue et al., 2004).

This study intends to investigate the importance of model parameter values in Sahelian simulations and to explore procedures in improving their estimation. Our approach is in line with MOPEX strategy (Figure 1 in Duan et al., this issue), which includes preparing data, estimating a priori parameters, conducting control model runs, calibrating parameters, conducting calibrated model runs, comparing results, and finally develop improved a priori parameter estimates. Our ultimate goal is to facilitate more realistic simulation of land/atmosphere interactions for use with coupled atmosphere/land models. These coupled models, whether general circulation models (GCMs) or regional models, may be used to study the impact of environmental threats such as deforestation and desertification.

This study focuses on the Sahel region in Africa. Because it is the transition zone between the dry Sahara Desert to the north and the tropical rain forest to the south, the Sahel has a very sensitive climate system, making it a good subject for climate study. Furthermore, in at least the past 25 years, there has been a severe drought, which has brought famine to

many residents of the area. This desertification problem in the Sahel underscores the importance of the study of land surface climate interaction.

A number of studies have demonstrated the importance of a single land surface variable to the Sahelian climate using simple land models (e.g. Walker and Rowntree, 1977; Sud and Fennessy, 1982; Laval and Picon, 1986; Kitoh et al., 1988). Furthermore, the importance of synthetic vegetation/soil conditions in the Sahelian climate was assessed in coupled atmosphere and vegetation models (e.g. Xue and Shukla, 1993; Xue, 1997; Liu et al., 2004). In these studies, the vegetation types were changed over the specified study region, significantly altering the energy and water balance in the desertification run. Summer rainfall was reduced in the desertified area and increased to the south of the area. The surface air temperature was increased under desertified conditions, and the runoff and soil moisture were all reduced. These changes in temperature and precipitation were of the same level of magnitude as the anomalies that occurred during the last 40 years. However, in these studies, many surface parameters were changed in accordance with the changes in vegetation type. To better understand the mechanisms controlling interactions and gain better simulations of surface hydrology, it is desirable to further examine the roles of individual vegetation and soil parameters used by biosphere models to simulate land surface processes.

This paper makes use of data from two experiments conducted in the Sahel in the late 1980s and early 1990s: the Sahelian Energy Balance Experiment (SEBEX) (Wallace et al., 1991) and the Hydrological Atmospheric Pilot Experiment (HAPEX-Sahel) (Goutorbe et al., 1994). According to Wallace et al. (1991), data describing Sahelian vegetation was very sparse. Therefore, information about the energy and water balances in the Sahel was urgently needed. SEBEX was conducted with the goal of attaining direct measurements of surface energy fluxes from varying Sahelian land types. HAPEX-Sahel was conducted in Niger, West Africa, in 1991–1993 with the purpose of improving parameterizations of land surface atmosphere interaction on the scale of a GCM grid box. It was undertaken by scientists from several countries in order to study the energy and water balances on a regional scale. Part of the experiment

was the collection of measurements that could be used to examine the temporal and spatial characteristics of the boundary layer in the Sahel (Dolman et al., 1995).

SEBEX data have been used to evaluate the performance of several models, including the United Kingdom Meteorological Office (UK Meteo) GCM and the European Center for Medium range Weather Forecasting (ECMWF) model, in simulating the Sahelian climate. A one-dimensional version of the UK Meteo GCM was used to analyze hourly and daily performance, and the three-dimensional GCM was tested with monthly average data. The model overestimated monthly solar radiation by 20% during the dry season. It also overestimated monthly evaporation at the start of the wet season and underestimated it during the dry months (Dolman and Gregory, 1992; Dolman et al., 1993). Analysis of the one-dimensional version of the ECMWF model facilitated focus on the land surface–atmosphere parameterizations, and comparison of daily evaporation with observations indicated that adjustments to conductance in the model were necessary for agreement with observations (Gash et al., 1991).

Several studies have also utilized HAPEX-Sahel to explore the key processes at the land surface–atmosphere interface that have major impact on simulations in arid climates. Hanan and Prince (1997) derived empirical relationships to describe the climatic control of stomatal conductance for the common vegetation species in the HAPEX-Sahel area. They showed that, in general, the climatic variables that have the greatest impact on stomatal conductance are photosynthetically active radiation, vapor pressure deficit, and soil water potential. Blyth (1997) focused on the heterogeneous nature of the Sahelian landscape, noting that the semi-arid climate does not support full vegetation cover. Blyth demonstrated that spatial averages of surface parameters over a heterogeneous landscape can accurately represent evaporation over mixed vegetation types. Taylor et al. (1997) used HAPEX-Sahel to examine the impact of precipitation variability on the surface and atmosphere, exploring land surface feedback on rainfall at a regional scale. Their analysis of the data indicated that soil moisture patterns acted as a feedback mechanism affecting rainfall. In 2000, Taylor and Blyth went on to determine that evaporation from bare soil was a key component

affecting spatial variability of evaporation during the wet season, while leaf-level transpiration was consistent and not highly affected by soil moisture.

In this paper, we further investigate the parameterizations of vegetation and soil that are crucial for simulations of land surface climate interaction in the Sahel. Using a biophysical model, the Simplified Simple Biosphere Model (SSiB) (Xue et al., 1991), with different parameterizations and comparing the simulated results with observational data, this study provides further understanding of the mechanisms affecting the water and energy balance in the Sahel and will also identify which parameter values/parameterizations may be more important, and which values may be more proper, for simulations in this region. We believe the approach presented in this paper provides useful information in support of the purpose of MOPEX in guiding the development of better parameter estimates for model studies.

In this paper, Section 2 describes the SEBEX and HAPEX-Sahel data sets and uses these data to illustrate the climate of the Sahel. Section 3 examines the energy balance based on available observational data from both of these data sets. Section 4 describes the control model runs with both data sets, using standard type-8 (shrubs with ground-cover) parameters typically used to describe the land surface in the Sahel (see Dorman and Sellers, 1989, for an explanation of how standard vegetation parameters were compiled.). Section 5 makes use of the SEBEX data, which cover a 2-year period, for a sensitivity study of the surface parameters to be modified in the calibration. Section 6 uses the complete observations from HAPEX-Sahel for calibration of the surface parameters and the SEBEX data set for validation of those parameters. Conclusions are then summarized in Section 7.

2. Data sets and Sahel climate

SEBEX was conducted from late August 1988 through September 1990 by the UK Institute of Hydrology and the International Crops Research Institute for the Semi-Arid Tropics (ICRISAT). Near Niamey, Niger (13°15'N, 2°17'E), measurements were taken of all important driving climate factors (forcings), including incoming solar radiation,

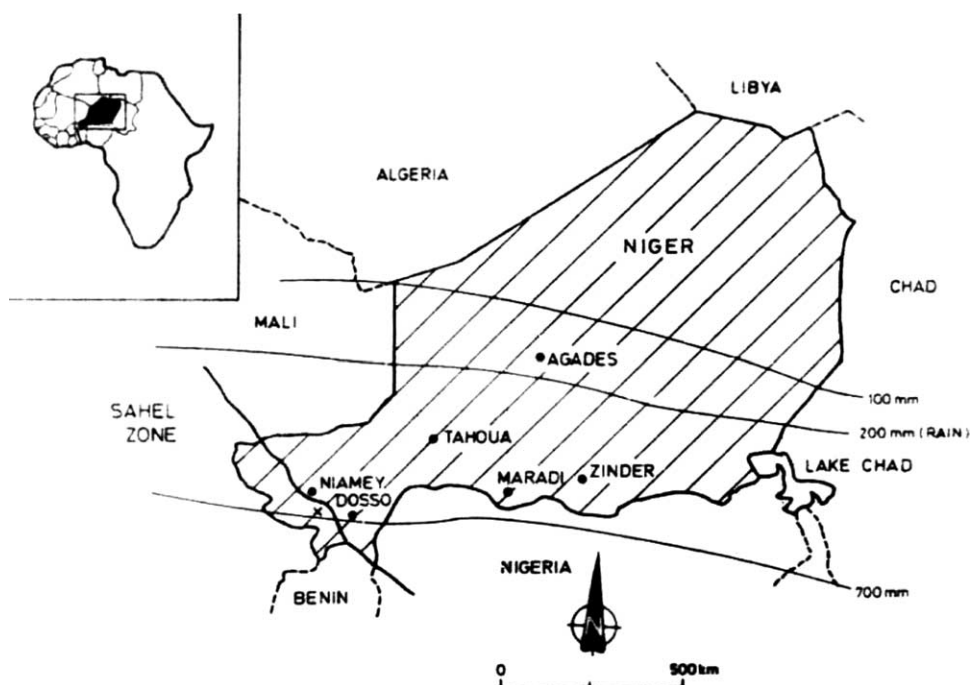


Fig. 1. Map of Sahel zone in relation to surrounding area.

downward long wave radiation, air temperature, vapor pressure, wind speed, and precipitation (Wallace et al., 1991). Fig. 1 shows the location of Niamey within Niger and the Sahel. In addition to the forcing variables, several other variables were recorded in the SEBEX. They include net radiation, latent heat flux, sensible heat flux, ground heat flux, surface temperature, friction velocity, and soil wetness fraction. Because the rainy season is the most critical part of the year to be studied in the Sahel, measurements for these variables were done most intensively during the summers, but they were not complete for the whole study period.

HAPEX-Sahel (Goutorbe et al., 1994) (referred to as HAPEX for the remainder of this paper) took place in the same region as SEBEX, but covered a larger area. Hydrological monitoring was conducted from 1991 to 1993 and covered sites on a scale of 100 km². A complete set of observations similar to those of SEBEX was taken during an 8-week intensive observation period from August 22, 1992, to October 9, 1992, which overlapped the end of the rainy season and the beginning of the dry season (Goutorbe et al., 1997). Because it contains more measured variables with little missing data, the shorter, intensive HAPEX

observation period is also utilized in this study. The original HAPEX measurements were 10-min averages, but we use hourly means in this study.

At the SEBEX site, 78% of the vegetation was comprised of leguminous and grass species (*Cassia mimosoides*, *Tephrosia linearis*, *Aristida mutabilis*, and *Eragrostis tremula*). The remainder was woody shrubs about 2.5 m in height (*Guiera senegalensis* and *Combretum glutinosum*) with a few occasional trees (1.5 per hectare) of 5–10 m in height. The soil tends to be very sandy and about 0.5 m deep. Measurements of latent heat (evaporation) and sensible heat fluxes were taken by eddy covariance instruments mounted on towers above the test site. Incoming solar radiation was measured by Kipp solarimeters. Infrared thermometers and automatic weather stations were used to record the other measurements (Wallace et al., 1991). Surface fluxes were measured in a similar manner for HAPEX.

Measurements of the SEBEX variables used for forcing were taken in hourly increments for 766 full days, starting August 26, 1988, and ending September 30, 1990. In a tropical region such as this, there is much cloud cover; so downward long wave radiation

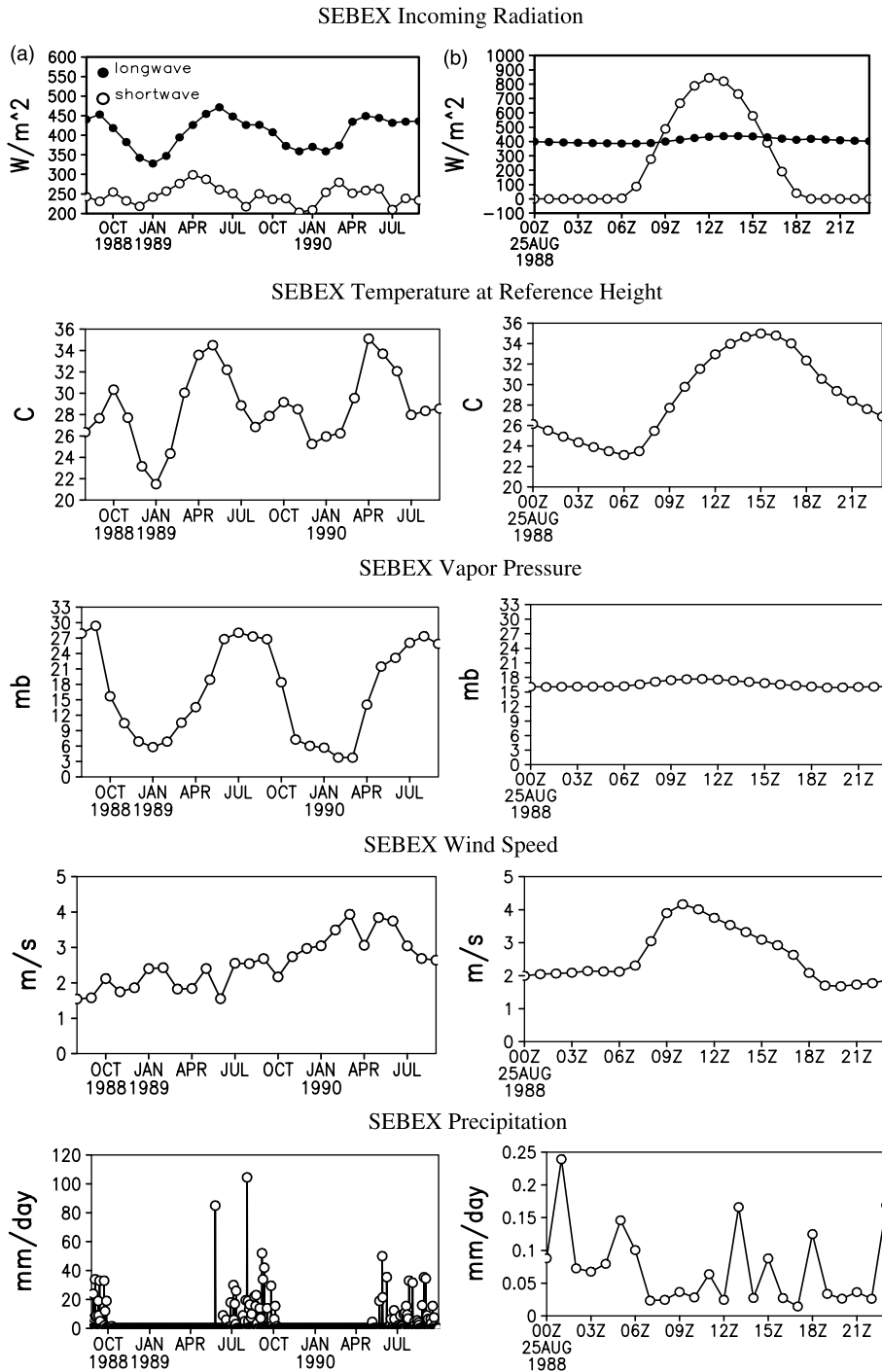


Fig. 2. (2.1) Incoming short-wave and long-wave radiation ($W m^{-2}$). (2.2) Temperature ($^{\circ}C$). (2.3) Vapor pressure (mb). (2.4) Wind speed ($m s^{-1}$). (2.5) Precipitation ($mm day^{-1}$) at SEBEX site as (a) monthly means and as (b) a diurnal cycle averaged over the entire observational period.

becomes the dominant source of incoming radiation. As shown in Fig. 2.1b, the short-wave radiation peaks at over 800 W m^{-2} , so it will be the primary source of incoming radiation for about six hours of the day, from 9 a.m. to 3 p.m.; but the long wave radiation, which deviates only slightly from its average of 408 W m^{-2} , has a higher average overall (Fig. 2.1a). The average incoming short-wave radiation is 246 W m^{-2} , which remains consistently below the long wave radiation during every month of the 2-year study. The net incoming radiation is greatest during the spring, before summer cloud cover begins to reduce the available solar radiation. The net incoming radiation is the least in the winter. HAPEX incoming radiation (not shown), measured largely during the month of September, is generally consistent with the range shown for SEBEX during that time of year, with long wave radiation dominant at about 434 W m^{-2} compared to short-wave radiation at 232 W m^{-2} . Similarly, the short-wave radiation during the day for HAPEX peaks at nearly 800 W m^{-2} .

Fig. 2.2 shows that the temperature at 10.75 m above the vegetation is correlated with the incoming radiation. It tends to be at a minimum during winter and then peaks in the spring before gradually reducing through the summer and autumn. The diurnal cycle shows a delayed response to incoming radiation during the day, with the maximum temperature of $35 \text{ }^\circ\text{C}$ occurring a few hours after the solar radiation peak, due to surface heating. From that point, the temperature gradually decreases to $23 \text{ }^\circ\text{C}$ at dawn. The average temperature over the 2-year study period is about $28.7 \text{ }^\circ\text{C}$, while during the shorter HAPEX period; the average is nearly $28 \text{ }^\circ\text{C}$. Fig. 2.3 shows the vapor pressure varying little during a day, but varying significantly seasonally. It reaches a minimum in January near 5 mb but a maximum during the summer between 25 and 30 mb. The wind speed, shown in Fig. 2.4, follows a clear diurnal cycle, with winds picking up quickly during the morning hours after sunrise, reaching over 4 m s^{-1} , and then declining steadily during the afternoon. At night, the wind speed remains fairly constant around 2 m s^{-1} . The pattern throughout the 2 years is variable, with an average of slightly over 2.5 m s^{-1} , which is comparable to forcings from HAPEX.

The rainy season in the SEBEX is generally during the summer, when cloud cover is greatest. The SEBEX test site shows the rainy season occurring

from May through October, with the most precipitation occurring during the summer months (Fig. 2.5a). Precipitation may occur at any time during the day, though the largest portion occurs during the nighttime (Fig. 2.5b). The HAPEX data, occurring near the end of the rainy season in 1992, contain two separate weeks with moderate rainfall events—one in late August and one in mid-September.

3. Energy balance from observational data

In the SEBEX forcing data, the net radiation tends to be smallest during the winter. It gradually increases through spring and into summer, and then declines again in autumn, consistent with the pattern of incoming radiation shown in Fig. 2.1a. The sensible heat flux is directly dependent upon the amount of net radiation available, such that during dry months it accounts for nearly all of the net radiation. However, during the wet months, the latent heat flux becomes dominant due to available water, and more than half of the net radiation is lost through evaporation.

Because SEBEX flux measurements were only taken thoroughly during the summer months, the energy balance is not complete throughout the entire study period. Based on daily mean values that were obtained only when no energy balance components were missing, an average of 123.1 W m^{-2} of net radiation was observed in the SEBEX area during the study period. Of this amount, 78.1 W m^{-2} , or about 63%, becomes latent heat, while 57.8 W m^{-2} becomes sensible heat and 7.4 W m^{-2} becomes ground heat flux. As shown in Table 1, the sum of the observed heat flux components (latent heat flux + sensible heat flux + ground heat flux) is 20.2 W m^{-2} more than the measured net radiation. Since the long-term mean of the ground heat flux should be close to zero, the mean value of 7.4 W m^{-2} is very likely caused by errors in measurements. The root-mean-square (RMS) error between the net radiation and the sum of the heat flux components is 24.7 W m^{-2} .

The HAPEX run, covering only about two months, shows a similar amount of net radiation. The measured net radiation is 126.9 W m^{-2} , compared with 124.4 W m^{-2} as the sum of the heat flux components. Thus there is less discrepancy during

Table 1
Observed energy balance (W m^{-2})

	Net Rad	LH	SH	GH	LH+SH+GH	RMS error	Observations
HAPEX	126.9	100.1	24.7	-0.4	124.4	9.94	49
SEBEX	123.1	78.1	57.8	7.4	143.3	24.7	148

Note: Observed energy balance components, based on daily mean values obtained only when all energy balance components were available, in which Net Rad is net radiation, LH is latent heat flux, SH is sensible heat flux, and GH is ground heat flux.

the shorter HAPEX observational period. There was less uncertainty in ground heat flux measurements, which were taken at 5 cm below the surface as compared to 2 cm in SEBEX. With a 5-cm temperature probe to estimate heat storage between 0 and 10 cm, the ground heat flux was probably measured more accurately in HAPEX than in SEBEX. In HAPEX, the latent heat flux accounts for 100.1 W m^{-2} , or nearly 79% of the measured net radiation. The sensible heat flux is 24.7 W m^{-2} , while ground heat flux is negligible at -0.4 W m^{-2} . Although the difference in observations is only 2.5 W m^{-2} , the RMS error is 9.94 W m^{-2} .

4. Control runs

The experiments described utilize the Simplified Simple Biosphere Model (SSiB) (Xue et al., 1991) to analyze the surface fluxes and other surface characteristics. The SSiB, which is a simplified version of the Simple Biosphere Model (SiB) developed by Sellers et al. (1986), is a biophysically based model of land-atmosphere interactions and is designed for global and regional studies (Xue et al., 1997). The model simulates the biophysical processes that occur at the land surface as a reaction to climatological conditions. It describes the surface in terms of one vegetation layer (reduced from two in SiB) and three soil layers. Water is received by the soil layers from precipitation or melting snow. This water stored by the soil may be evaporated by bare soil or transpired through the canopy. Surface runoff may occur at the top soil layer, and subsurface runoff may occur at the bottom soil layer. When a soil layer becomes saturated, it will also produce runoff. The total amount of water and energy entering and leaving the system will always remain balanced.

Bare soil evaporation has been found to be an important feature of the water and energy balance of

the Sahel (Taylor and Blythe, 2000). The evaporation from the ground is calculated in the SSiB by

$$E_s = [f_h q(T_{gs}) - q_a] / (r_{\text{surf}} + r_d),$$

in which f_h is the relative humidity of air at the soil surface, $q(T_{gs})$ is the saturated specific humidity at the surface temperature, q_a is the specific humidity at the canopy air space, r_{surf} is the bare soil surface resistance, and r_d is the aerodynamic resistance between the canopy air space and the ground (Xue et al., 1996a,b).

In this paper, off-line tests are conducted, meaning that the SSiB land surface scheme is not linked to any GCM or regional model—the prescribed atmospheric conditions are already determined for each time step of the model run. These variables, known as forcings, are obtained from field measurements from SEBEX and HAPEX-Sahel and are used to drive the model. SSiB calculates the resulting surface energy fluxes as well as other predictive variables, such as soil wetness fraction at each of three layers, runoff (including surface runoff and sub-surface runoff, or drainage), canopy water content, snow cover (not applicable in this study), and surface and deep soil temperatures. This type of study evaluates the land surface scheme and does not incorporate the feedbacks that would occur as a result of these fluxes.

Because HAPEX observations were taken intensively for 8 weeks, producing a complete set of flux measurements for the whole study period, the HAPEX set was used for model parameter calibration (Section 6). The SEBEX set contains 2 years of forcing data and was used for validation (Section 6) and sensitivity testing (Section 5) to guide/evaluate the calibration process. The control run for HAPEX (referred to as H-1) employed parameters for standard type-8 vegetation (Table 2), shrubs with ground-cover (Dorman and Sellers, 1989), which is normally used in GCMs for the Sahel area. SSiB is a one-layer

Table 2
Vegetation and soil parameters in control and experimental runs

Vegetation and soil parameters		Control/Type-8 (H-1 and S-1)	New (H-2 and S-2)
Leaf area index	August	0.808	1.508
	September	1.508	2.008
	October	1.148	0.622 (starting Sept. 21)
Minimum stomatal resistance ($s\ m^{-1}$)		1097	81.5
Vegetation height (m)		5	5
Roughness length (m)	August	0.267	0.267
	September	0.292	0.292
	October	0.280	0.280
Soil depth (m)	Layer 1 (top)	0.02	0.02
	Layer 2	0.47	0.47
	Layer 3	1.00	1.00
Wilting point		0.272	0.272
Hydraulic conductivity at saturation ($m\ s^{-1}$)		0.176×10^{-3}	6.9×10^{-3}
Thermal diffusivity ($m^2\ s^{-1}$)		5.0×10^{-7}	2.5×10^{-7}

vegetation model. For two-story vegetation types such as type-8, some parameters, such as LAI, are the sum of values at two layers, while others, such as minimum stomatal resistance, are weighted averages of the two layers. However, aerodynamic resistance and albedo are calculated separately in preprocesses in which a two-story structure is preserved (see Xue et al., 1991, for more detail).

A control run with SEBEX data (referred to as S-1) with type-8 parameters was also conducted for comparison. Table 3 summarizes the simulated averages for control runs in comparison to observations, and Table 4 summarizes the corresponding root-mean-square errors, based on daily averages. For consistency when comparing to observations, the modeled energy balance components in these tables are calculated from values existing at the same time steps as used for Table 1, when all observed energy balance components were available. Calculations for

surface temperature and friction velocity are done with all daily values concurrent with existing observations.

In H-1, the average modeled latent heat flux (Fig. 3a) is $25.2\ W\ m^{-2}$ lower than the average observed value of $100.1\ W\ m^{-2}$, while the average modeled sensible heat flux (Fig. 3b) is $31.2\ W\ m^{-2}$ higher than the average observations of $24.7\ W\ m^{-2}$. While both fluxes are close to observations during the night hours (Fig. 4a and b), most of the inconsistency occurs during the day when net radiation (not shown) is greatest. Average ground heat flux (Figs. 3c and 4c) is $4.5\ W\ m^{-2}$ higher than the observed average of $-0.4\ W\ m^{-2}$. Modeled surface temperature (Fig. 3d) is quite close to observations, at 29.6 versus $29.1\ ^\circ C$; however, the temperature is overestimated by as much as $4\ ^\circ C$ during the day and underestimated by 1° or $2\ ^\circ C$ during the night (Fig. 4d). The friction velocity (not shown) follows the same diurnal pattern as the wind speed in Fig. 2.4b. The average friction

Table 3
Observed and simulated averages from HAPEX and SEBEX runs

		LH ($W\ m^{-2}$)	SH ($W\ m^{-2}$)	GH ($W\ m^{-2}$)	T ($^\circ C$)	U^* ($m\ s^{-1}$)
HAPEX	Measured	100.1	24.7	-0.4	29.1	0.19
	H-1	74.9	55.9	4.1	29.6	0.21
	H-2	101.5	28.3	6.6	29.3	0.21
SEBEX	Measured	78.1	57.8	7.4	29.9	0.26
	S-1	36.3	75.7	1.2	30.9	0.26
	S-2	56.1	53.5	2.2	31.2	0.27

Note: Observed and simulated averages from HAPEX and SEBEX Runs, in which LH is latent heat flux, SH is sensible heat flux, GH is ground heat flux, T is surface temperature, and U^* is friction velocity.

Table 4
Root-mean-square error in observations and simulations

		Obs Net Rad (W m^{-2})	LH (W m^{-2})	SH (W m^{-2})	GH (W m^{-2})	T ($^{\circ}\text{C}$)	U^* (m s^{-1})
HAPEX	H-1	9.94	27.3	32.7	5.83	1.06	0.028
	H-2		11.5	11.8	10.5	1.20	0.028
SEBEX	S-1	24.7	48.2	30.6	8.56	1.39	0.053
	S-2		29.6	18.2	9.55	1.50	0.051

Note: Root-mean-square error in observations and simulations, in which LH is latent heat flux, SH is sensible heat flux, GH is ground heat flux, T is surface temperature, and U^* is friction velocity.

velocity is 0.21 m s^{-1} , close to observations of 0.19 m s^{-1} . With root-mean-square errors of 27.3 and 32.7 W m^{-2} , respectively, the simulated errors for latent and sensible heat flux are significantly greater than the discrepancy in HAPEX observational data of 9.94 W m^{-2} . We will refer to this discrepancy as observational error in the rest of the paper.

Fig. 5a shows the observed accumulation of water balance components during the study period, and Fig. 5b shows the accumulated water balance

components of run H-1 for comparison. The runoff in Fig. 5a was derived based on the water balance using observed precipitation, evaporation, and soil moisture change. As rainfall occurs on several occasions, accumulating eventually to 182 mm , evaporation is taking place at a steady rate in both the observations and the simulation. However, by the end of the study period, simulated evaporation is underestimated, reaching only 130 mm (Fig. 5b) compared with 174 mm according to observations

HAPEX-Sahel (1992)

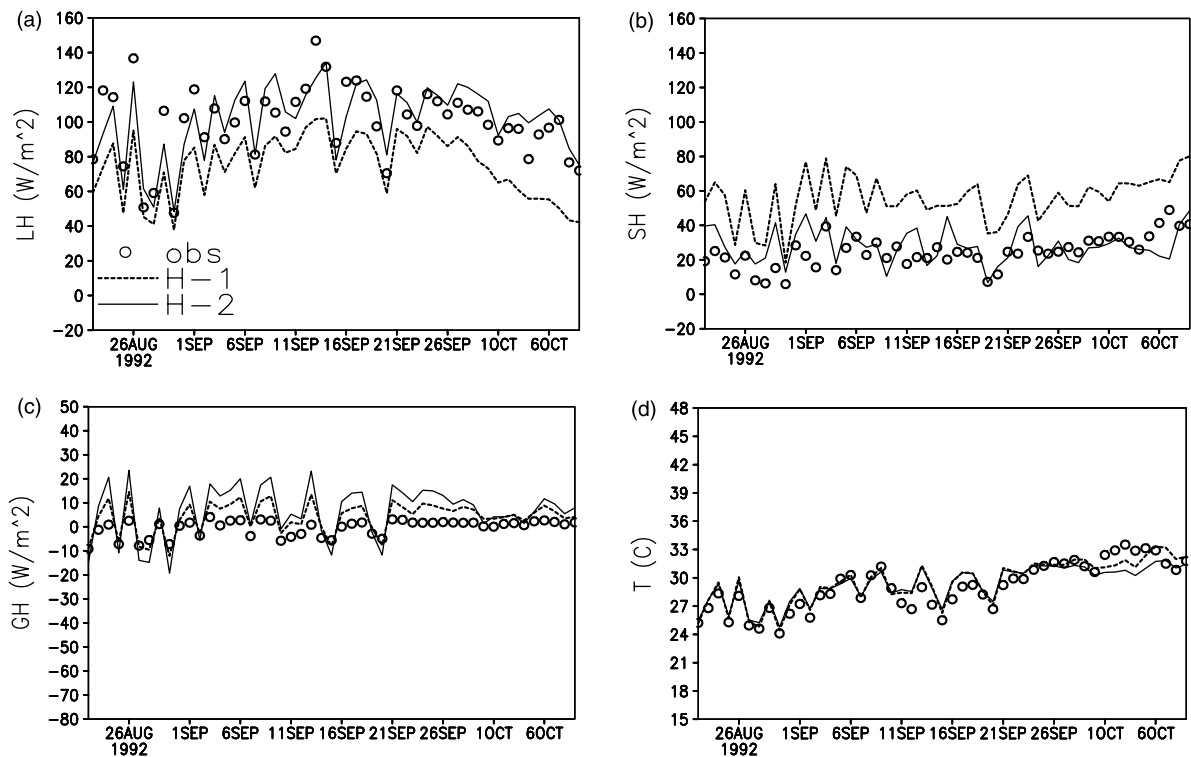


Fig. 3. Daily observed and simulated (a) latent heat flux (W m^{-2}), (b) Sensible heat flux (W m^{-2}), (c) Ground heat flux (W m^{-2}), (d) Surface temperature ($^{\circ}\text{C}$) with HAPEX-Sahel forcing.

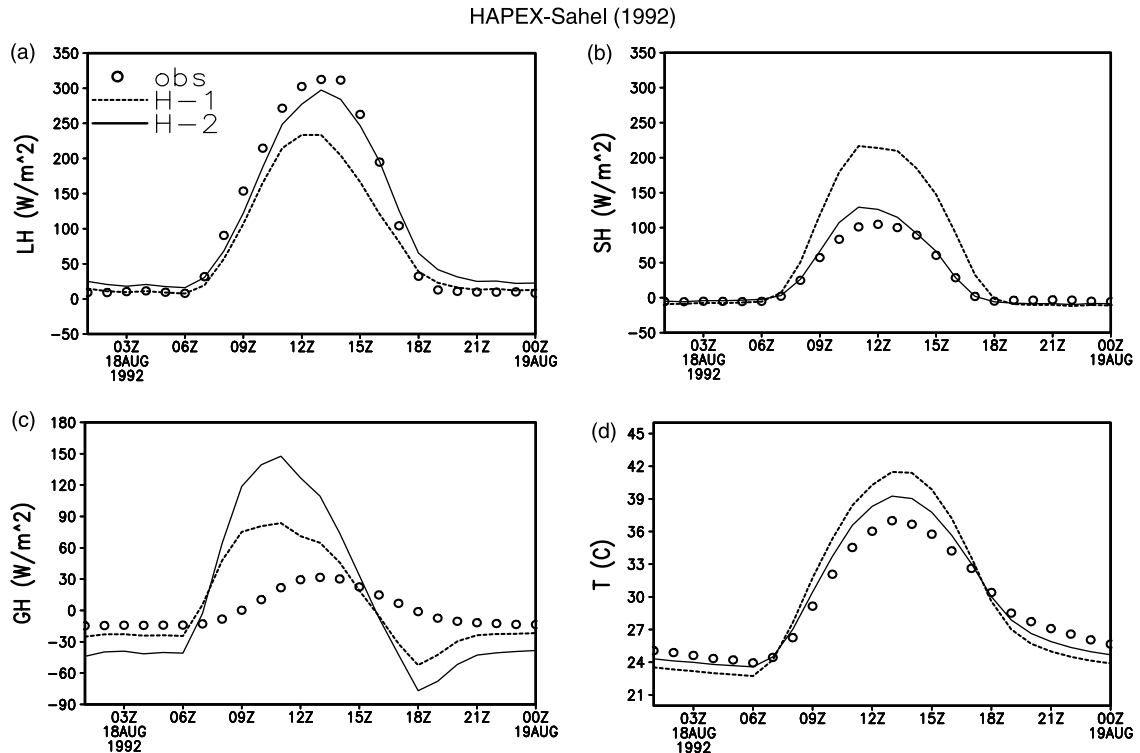


Fig. 4. Diurnal cycle of observed and simulated (a) latent heat flux (W m^{-2}), (b) sensible heat flux (W m^{-2}), (c) ground heat flux (W m^{-2}), and (d) surface temperature ($^{\circ}\text{C}$) with HAPEX-Sahel forcing.

(Fig. 5a). Since this period was primarily dry, soil moisture decreases whenever no rain occurs. In H-1, not much moisture was lost at all during this time frame—only 12 mm (Fig. 5b) compared with 112 mm according to observations (Fig. 5a). At the first layer (0–2 cm), only 6 mm are lost at the first layer (Fig. 5b), compared with 57 mm observed (Fig. 5a). The timing of the runoff (which includes surface runoff and drainage) is linked to precipitation events. Runoff in H-1 (Fig. 5b) is severely underestimated at 63 mm, compared with 120 mm (Fig. 5a), primarily due to underestimation of drainage.

The SEBEX control run (S-1) shows similarity with the HAPEX control run (H-1). The measured net radiation is 20.2 W m^{-2} lower than the sum of the measured heat flux components. But this observational error cannot account for simulated latent heat flux (Figs. 6a and 7a) being 36.3, 41.8 W m^{-2} lower than 78.1 W m^{-2} observed. The error for the simulated sensible heat flux (Figs. 6b and 7b) is also quite large, 75.7 W m^{-2} , being

17.9 W m^{-2} higher than the observed value of 57.8 W m^{-2} . While the SEBEX observational RMS error is greater than that of HAPEX, at 24.7 W m^{-2} , the RMS errors for simulated latent and sensible heat flux are 48.2 and 30.6 W m^{-2} , respectively. Fig. 7a and b again shows the main difference to occur during the day, when net radiation is greatest. Simulated ground heat flux (Figs. 6c and 7c) is 6.2 W m^{-2} lower than the observed average of 7.4 W m^{-2} . Since ground heat flux generally has an average close to zero, the observations may be more uncertain in this case (as discussed earlier) than the simulation. Modeled surface temperature (Figs. 6d and 7d) is 1.0°C higher than observations, at 30.9 versus 29.9°C . Modeled friction velocity (not shown) follows a similar pattern to that in H-1. In this case, there is essentially no difference in the average friction velocity. Fig. 8 shows a comparison of the soil wetness between 5 and 50 cm for the observations and between 2 and 49 cm for the control (S-1) run. The average soil wetness during the control

HAPEX-Sahel (1992)

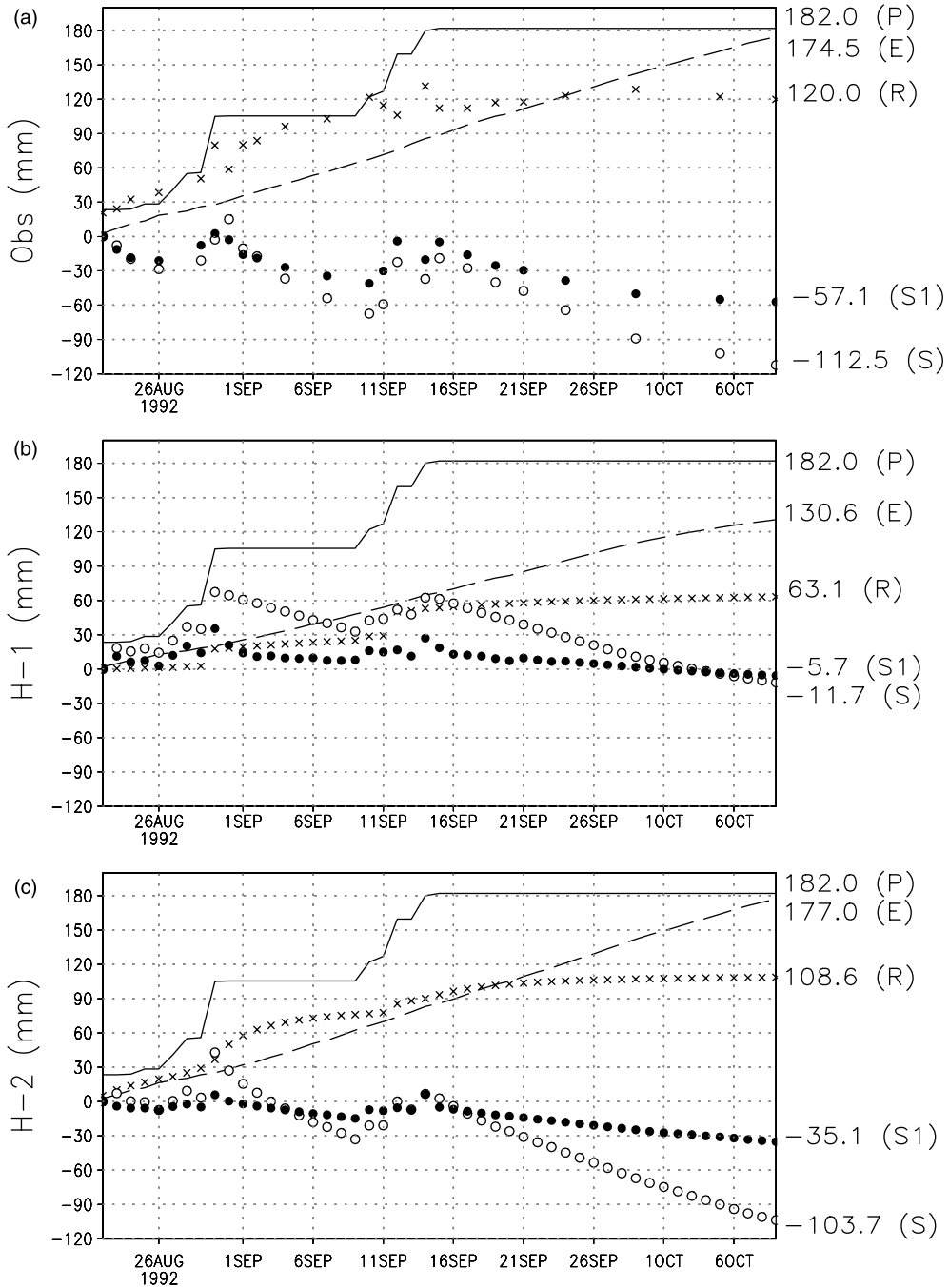


Fig. 5. Accumulated precipitation (P), evaporation (E), total runoff (R), and the change of total (S) and first layer (S1) soil water contents (all in mm) from their values on the first day, with HAPEX-Sahel forcing.

simulation is at times twice as high as observed, with a wetness fraction of 0.37 compared to 0.18.

By and large, the model produces reasonable diurnal and seasonal variations of fluxes, temperature, and soil moisture, but with substantial discrepancies in the means, RMS errors, and maximums and minimums within the diurnal cycle. Since the vegetation and soil parameters (Table 2) used for H-1 and S-1 were from a table, which is not based on the surface conditions at the SEBEX or HAPEX sites, we decided to calibrate these parameters to examine whether better assignment of these parameters would substantially improve the simulation.

5. Sensitivity testing

In order to calibrate the land surface parameters, numerous sensitivity tests with SEBEX data, which contain climate forcing for over 2 years and therefore

incorporate seasonal differences in climatology, were conducted to determine the effects of various vegetation and soil parameters on the model results. Although each parameter caused alterations to the model results, tests showed that only a few had more substantial impact than the others. Although changing albedo had a major impact in the sensitivity tests, it was not desirable to alter this parameter in the calibration since the type-8 vegetation already represented an albedo similar to that observed at the HAPEX site. The primary parameters discussed in this section and adjusted in the final calibration are as follows: leaf area index (LAI), stomatal resistance, soil hydraulic conductivity at saturation, and soil thermal diffusivity. Based on varying values for each of these four parameters individually while holding all others constant, the average latent heat flux, sensible heat flux, runoff, and canopy air space temperature over the integration period are plotted in Figs. 9–12; each data point represents an average for the entire 2-year model run.

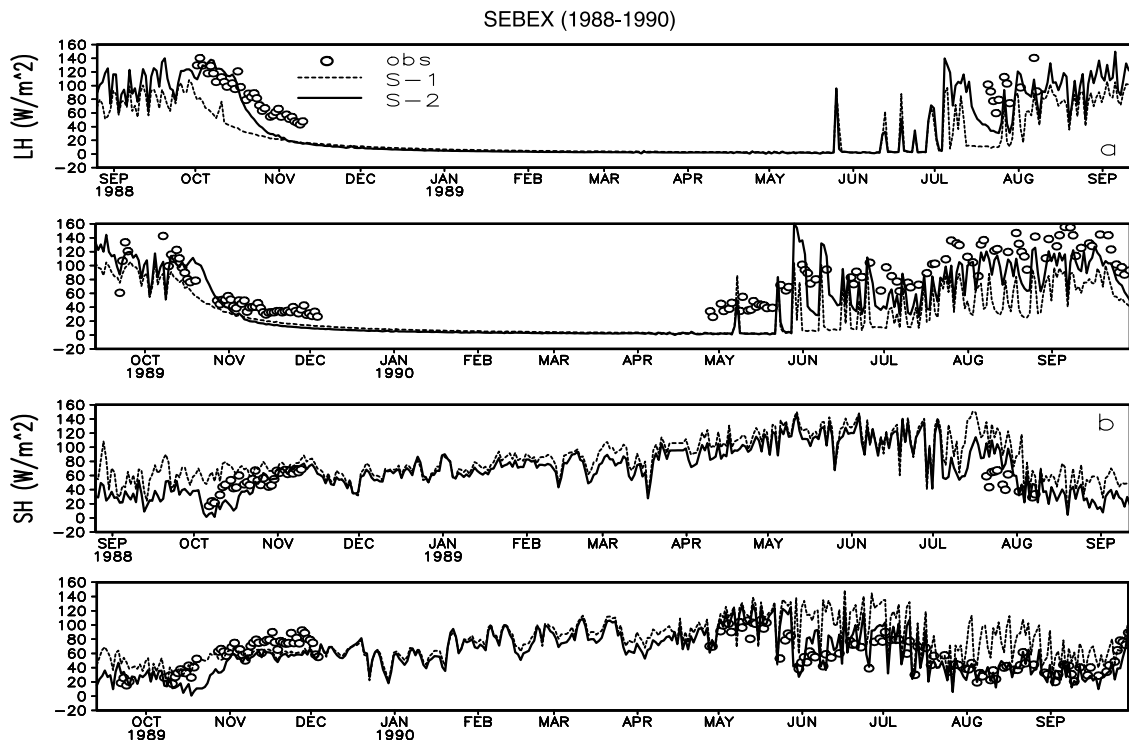


Fig. 6. Daily observed and simulated (a) latent heat flux (W m^{-2}), (b) sensible heat flux (W m^{-2}), (c) ground heat flux (W m^{-2}), and (d) surface temperature ($^{\circ}\text{C}$) with SEBEX forcing.

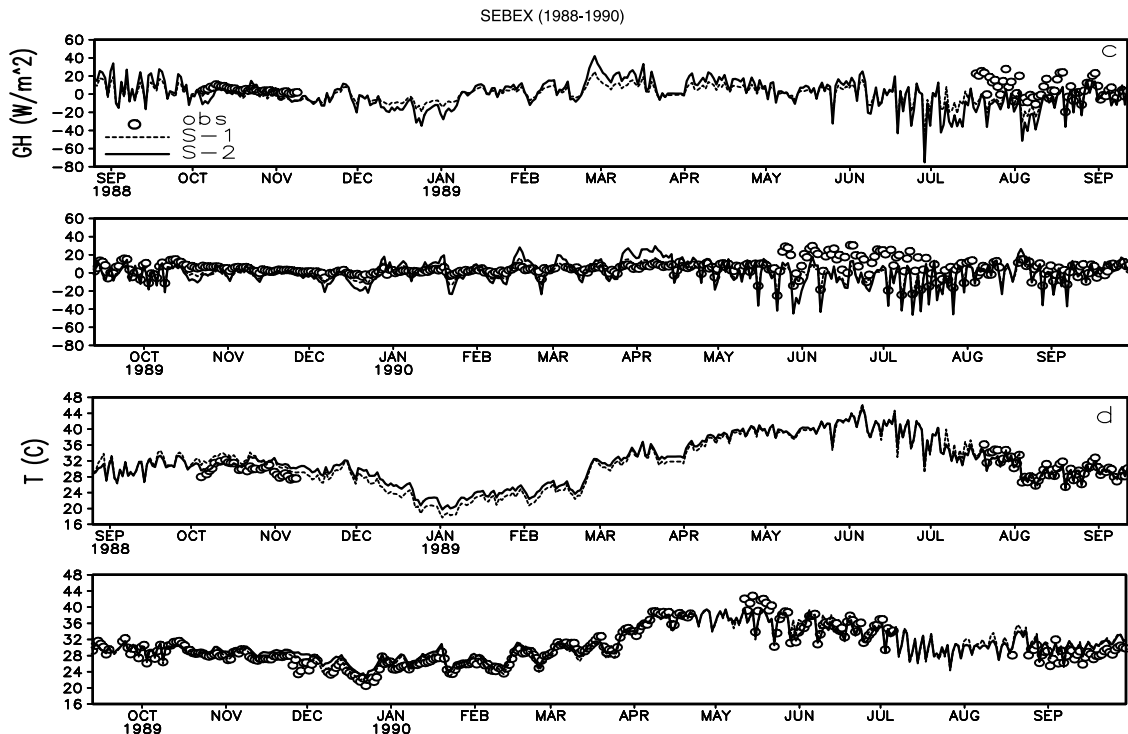


Fig. 6 (continued)

Among the parameters chosen for the calibration, LAI was one of the most dominant, as Xue et al. (1996) found in their off-line sensitivity study of vegetation parameters using data from the Anglo-Brazilian Amazonian Climate Observation Study (ABRACOS). In the semi-arid climate of the Sahel, greater LAI means the canopy provides more leaf area from which transpiration may occur. Also, more incoming energy may be absorbed, which may be used for evaporation. Above an LAI of 1.0, evaporation reaches a saturation point at which further increase in LAI has little impact on energy partitioning, but since the type-8 vegetation consists of LAI much less than 1.0, this parameter is significant for this study. Increasing LAI from 0 to 1.0 increases net radiation by about 14 W m^{-2} , most of which increases latent heat flux (Fig. 9a). As transpiration increases, the roots take up more water, drying the soil and reducing drainage. Runoff (Fig. 9c) is decreased from 0.50 to about 0.25 mm day^{-1} and toward 0.15 mm day^{-1} as LAI

approaches 5. Sensible heat flux (Fig. 9b) and canopy air space temperature (Fig. 9d) are affected minimally.

The other primary parameter with significant effect in the tests was stomatal resistance. Stomatal resistance in the vegetation canopy affects the amount of water vapor, carbon dioxide, and trace gases that may be exchanged between the leaves and the atmosphere (Hanan and Prince, 1997). Therefore, the stomata of plants play a central role in photosynthesis and evapotranspiration. In semi-arid environments such as the Sahel, where the rainy season may be short and variable, water regulation is particularly key to plant survival, making stomatal resistance an important parameter. The stomatal resistance affects the partitioning between latent and sensible heat flux. As less exchange of water vapor occurs as stomatal resistance varies from 0 to $10,000 \text{ s m}^{-1}$, latent heat flux (Fig. 10a) decreases by 8 W m^{-2} , while sensible heat flux (Fig. 10b) increases by that same amount. Since there is little

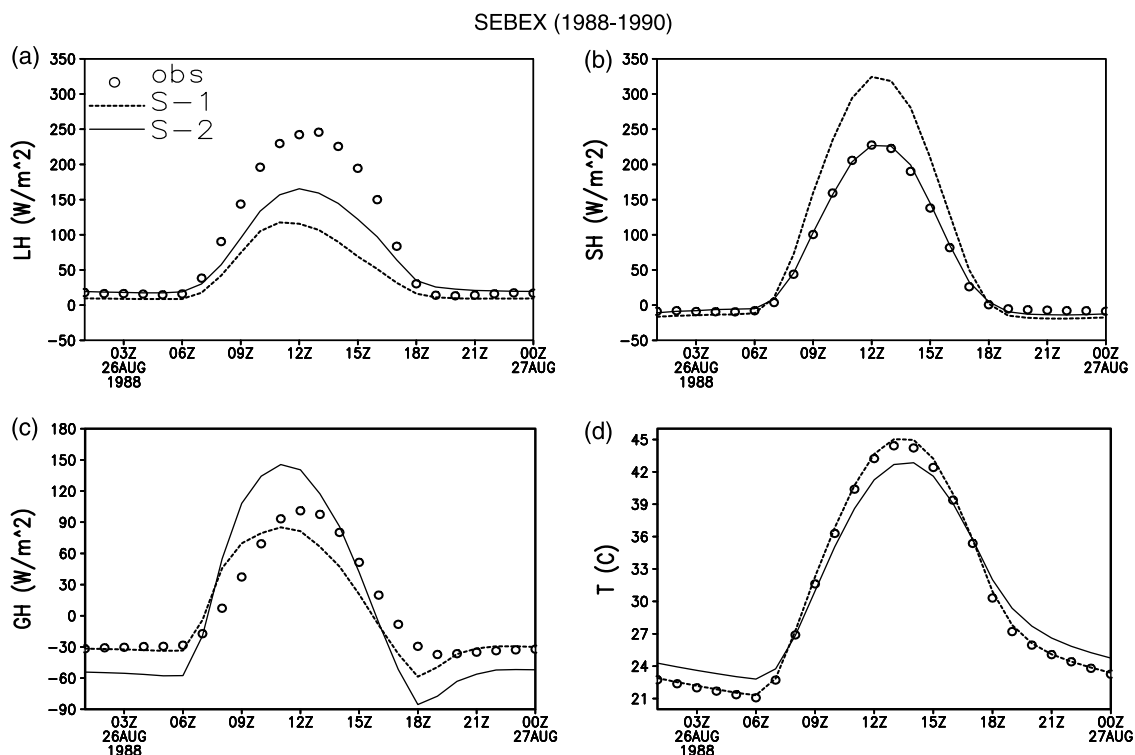


Fig. 7. Diurnal cycle of observed and simulated (a) latent heat flux (W m^{-2}), (b) sensible heat flux (W m^{-2}), (c) ground heat flux (W m^{-2}), and (d) surface temperature ($^{\circ}\text{C}$) with SEBEX forcing.

vegetation during the dry season, the actual impact of stomatal resistance during the rainy season is much higher than this number, which represents an average of all seasons. In general, the sensible heat flux is determined primarily by the available net radiation and secondarily by the amount of energy partitioned to latent heat flux. Runoff (Fig. 10c) responds in direct, inverse proportion to the change in evaporation. Both LAI and stomatal resistance have little impact on canopy air temperature. In off-line tests, surface temperature usually follows the temperature at reference height closely, except in some special cases as discussed below.

Oil hydraulic conductivity at saturation (Fig. 11) impacts the results as it is increased exponentially. Multiplying by a factor of 10, for example, may increase latent heat flux (Fig. 11a) by about 2 W m^{-2} while reducing sensible heat flux (Fig. 11b) by approximately the same amount. As moisture is absorbed more quickly into the soil surface, surface

runoff is reduced, and runoff (Fig. 11c) is reduced by as much as 0.05 mm day^{-1} . Canopy air space temperature (Fig. 11d) remains largely unchanged.

H-1 shows that the model has a systematic bias in simulation of surface temperature: cooler at night and warmer around noon (Fig. 4d). Since the previous tests (LAI, stomatal resistance, and soil hydraulic conductivity) showed little impact on these diurnal variations, the thermal diffusivity was tested to see whether this parameter has impact on the diurnal cycle of temperature. Although changing this parameter has little effect upon latent heat flux (Fig. 12a) or runoff (Fig. 12c), an increase such as changing from 2.5×10^{-7} to $5.0 \times 10^{-7} \text{ m}^2 \text{ s}^{-1}$ leads to an increase of over 4 W m^{-2} in sensible heat flux (Fig. 12b) and a decrease in surface temperature of more than $0.5 \text{ }^{\circ}\text{C}$ (Fig. 12d). As thermal diffusivity increases, soil heat capacity decreases, which leads to higher diurnal variation: higher canopy temperature in the daytime and lower

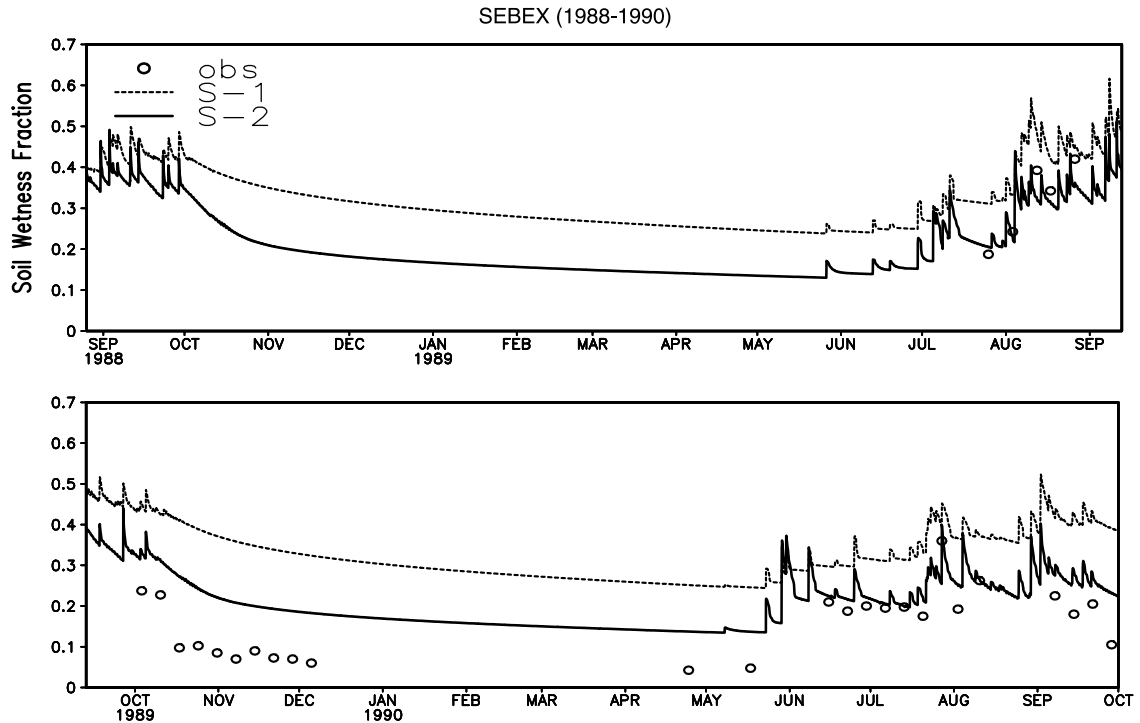


Fig. 8. Daily observed (5–50 cm) and simulated (2–49 cm) soil water content with SEBEX forcing.

canopy temperature at nighttime. In this site, the effect at nighttime is dominant and produces lower mean canopy air space temperature. Meanwhile, lower average upward long wave radiation due to lower surface temperature is compensated by higher mean sensible heat flux since downward total radiation remains the same. Sensible heat flux at night is small due to minimal net radiation. There is little difference with different diffusivity. Higher daytime sensible heat flux is consistent with higher daytime surface temperature. Further study shows that proper thermal diffusivity is crucial for correcting the bias and will be discussed later.

6. Calibration and validation

Based on the simulation errors in the control runs and the results of the sensitivity study, we gained a comprehensive idea of how to calibrate parameter values to make the simulation closer to observations. After identifying the key parameters that affect

the model simulation, few parameters were left for calibration. Furthermore, we would not do any calibration on variables that already have reliable measurements and are more stable, such as surface albedo (Allen et al., 1994). Tests were conducted to calibrate these remaining key parameters using the HAPEX data. Some measured SEBEX vegetation parameters (Wallace et al., 1991), such as LAI, were used to guide the process, and information from the sensitivity studies helped us to decide the direction of adjustment.

For this single site with limited key parameters, a couple of trial and error tests were sufficient to find an optimal set of parameter values. For a basin scale study with a large amount of grid boxes, a numerical optimization scheme would be necessary to complete the procedure. However, we believe the sensitivity studies, which identify the crucial parameters, may still be necessary to reduce the working load and to find the best parameter sets. The errors in the observational data sets (see Section 3) provide a standard for when calibration is sufficient. Table 2

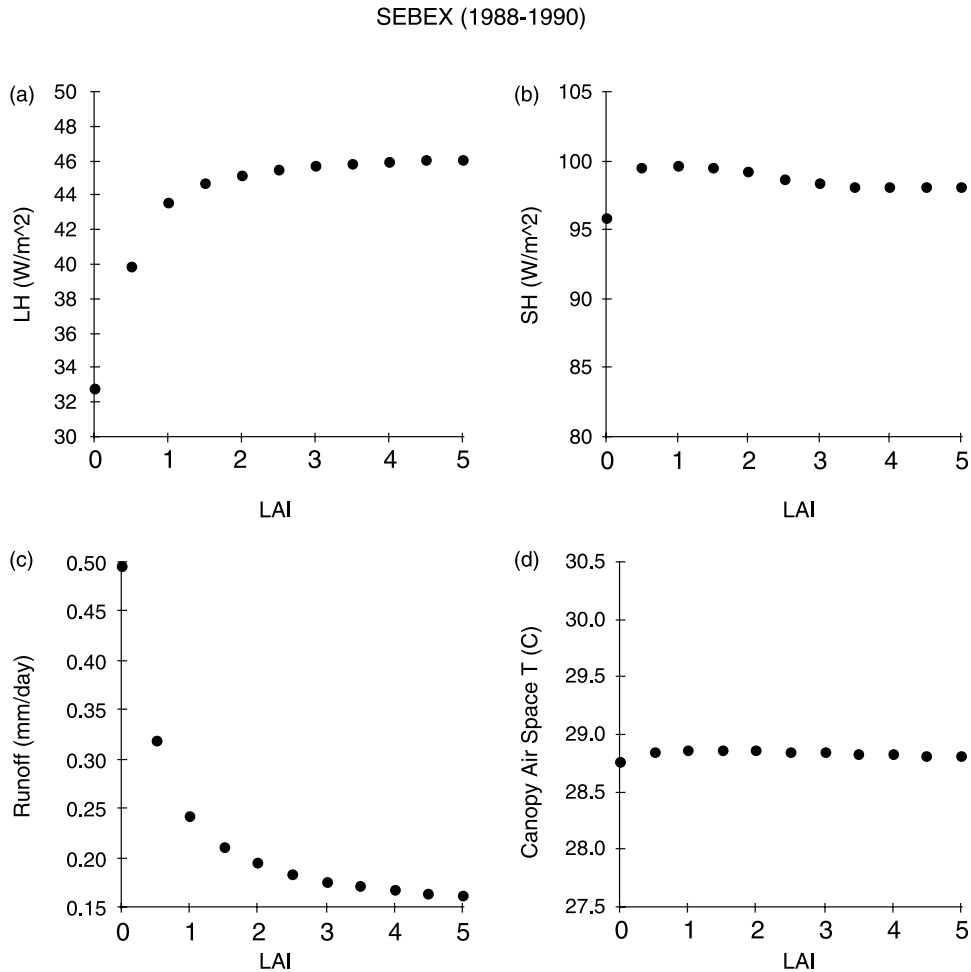


Fig. 9. Average (a) latent heat flux (W m^{-2}), (b) sensible heat flux (W m^{-2}), (c) runoff (mm day^{-1}), and (d) canopy air space temperature ($^{\circ}\text{C}$) over 2-year SEBEX period, varying by leaf area index.

displays the differences in surface parameters between the control and experimental runs.

Due to the high spatial and inter-annual variability of vegetation in this region, it is not surprising that not every measured value, such as SEBEX LAI, was suitable for the HAPEX run. For example, for the month of August, it was desirable to use a value (1.508, Table 2) higher than in either the type-8 set (0.808, Table 2) or SEBEX (1.162, Wallace et al., 1991). In the month of September, a value of 2.008 (Table 2) was used, as compared to 1.508 from type 8 (Table 2) or 1.352 from SEBEX (Wallace et al., 1991). This high degree of temporal variability demonstrates the sensitivity of the region to climate

and demonstrates the difficulty in choosing one set of vegetation parameter values to cover wide areas over different time periods. In the new data set, the minimum stomatal resistance in the calibrated data set is more than one order of magnitude lower. The hydraulic conductivity at saturation is more than one order of magnitude greater. Thermal diffusivity is cut in half.

The main problem in H-1 and S-1, as described in Section 4, was that latent heat flux was severely underestimated, especially during the daytime hours (Figs. 4a and 7a). By increasing the leaf area index for most of the run, more evapotranspiration was allowed to take place. Furthermore, by reducing

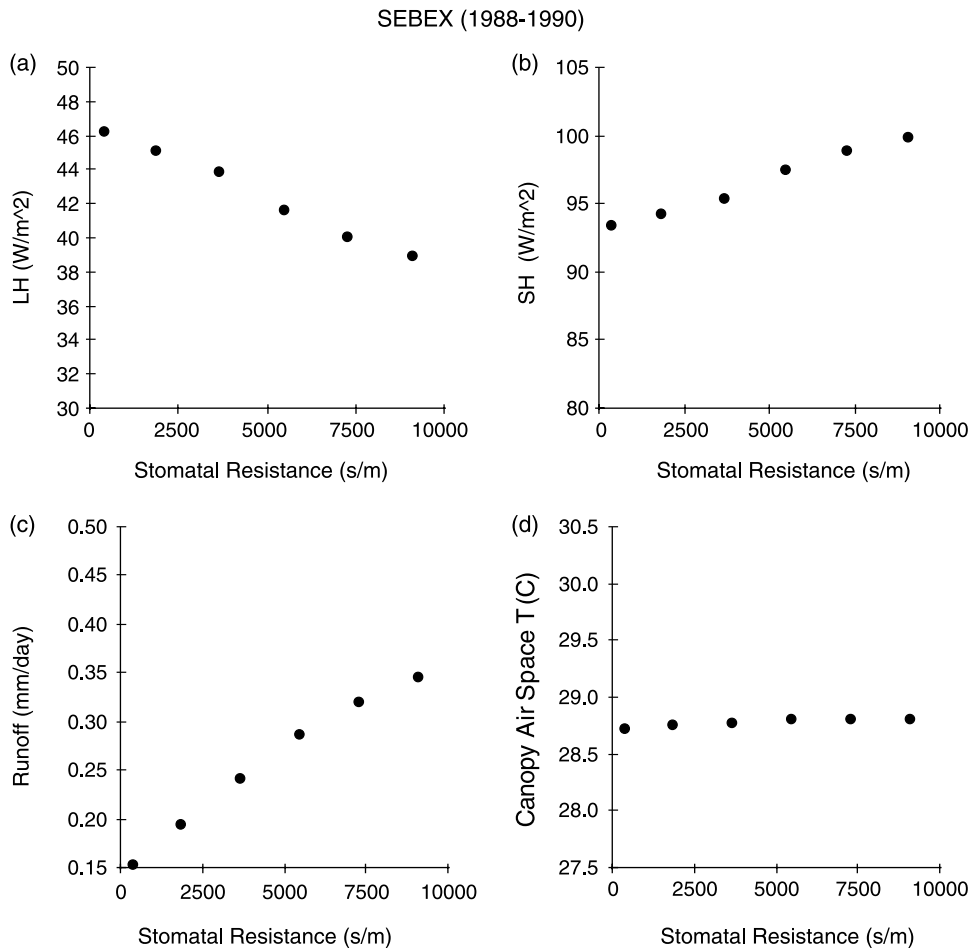


Fig. 10. Average (a) latent heat flux (W m^{-2}), (b) sensible heat flux (W m^{-2}), (c) runoff (mm day^{-1}), and (d) canopy air space temperature ($^{\circ}\text{C}$) over 2-year SEBEX period, varying by stomatal resistance (s m^{-1}).

the stomatal resistance, more exchange of water vapor was allowed to occur. These two changes, as demonstrated in the sensitivity studies, have the effect of increasing latent heat flux, bringing it closer to observations (Figs. 3a and 4a). As a result, the sensible heat flux, which was overestimated, is lowered (Figs. 3b and 4b). The decrease in thermal diffusivity also has a role in reducing the sensible heat flux without impacting the latent heat flux. In particular, by decreasing the thermal diffusivity, soil heat capacity increases, which leads to lower temperature in the daytime and higher temperature at nighttime (Fig. 4d).

Figs. 3–5 show significantly improved results for H-2. The averages for the simulated latent, sensible,

and ground heat fluxes change from 74.9 to 101.5 W m^{-2} , from 55.9 to 28.3 W m^{-2} , and from 4.1 to 6.6 W m^{-2} , respectively (Table 3). Thus, the average latent heat flux and sensible heat flux are much closer to their observed averages of 100.1 and 24.7 W m^{-2} , making the difference in latent heat flux negligible and the simulated sensible heat flux much closer to the observation. At 6.6 W m^{-2} , the average ground heat flux moved 2.5 W m^{-2} further away from the observed average of -0.4 W m^{-2} , but the total difference of 7 W m^{-2} still remains less than the observational RMS error of 9.94 W m^{-2} . The RMS errors reduced to 11.5 W m^{-2} for latent heat flux and 11.8 W m^{-2} for sensible heat flux, both now close to the observational error.

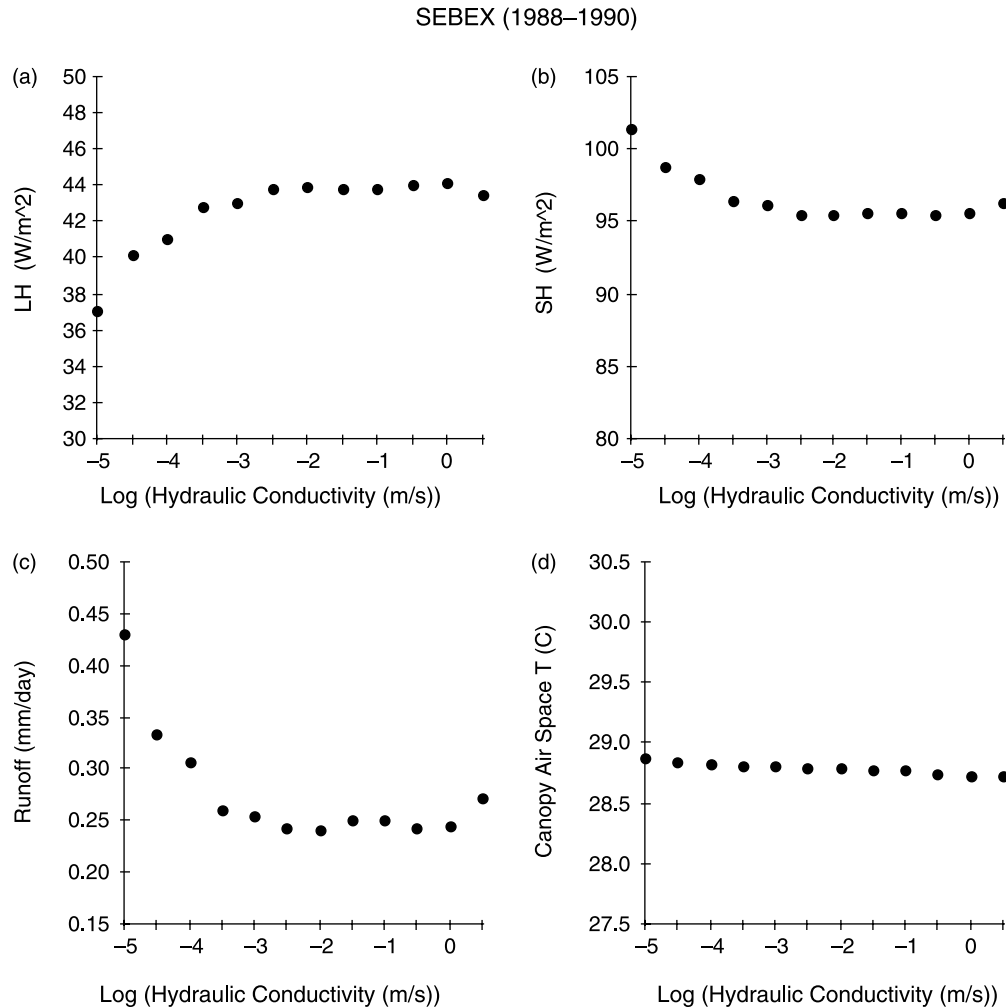


Fig. 11. Average (a) latent heat flux (W m^{-2}), (b) sensible heat flux (W m^{-2}), (c) runoff (mm day^{-1}), and (d) canopy air space temperature ($^{\circ}\text{C}$) over 2-year SEBEX period, varying by the logarithm of hydraulic conductivity at saturation (m s^{-1}).

The average temperature of H-2 was reduced by 0.3°C , but more importantly the daytime overestimation and nighttime underestimation were both reduced, as seen in Fig. 4d. The daily RMS error for surface temperature increased only slightly from 1.06 to 1.20°C . Friction velocity was not significantly affected by the calibration.

Fig. 5c shows the new accumulation of water for comparison with observations (Fig. 5a) and run H-1 (Fig. 5b). Now evaporation is much closer to observations, similarly rising steadily until reaching 177 mm , much closer to 174 mm observed. Now, like the observations, much moisture is lost from the soil,

104 mm by the end of the run compared with 112 mm observed, and 35 mm at the first soil layer compared with 57 mm observed. The calculated runoff rises to 109 mm , compared with 120 mm observed.

The new data set was validated with the two-year SEBEX simulation (S-2). These results are plotted in Figs. 6–8. Figs. 6a and 7a show that the new data set leads to an improvement in the simulation of latent heat flux. The observations peak at noon or 1 p.m. (Fig. 7a), with an average of 78.1 W m^{-2} . Whereas run S-1 severely underestimates the average latent heat flux with an average of only 36.3 W m^{-2} , run S-2 improves the average to 56.1 W m^{-2} . The RMS

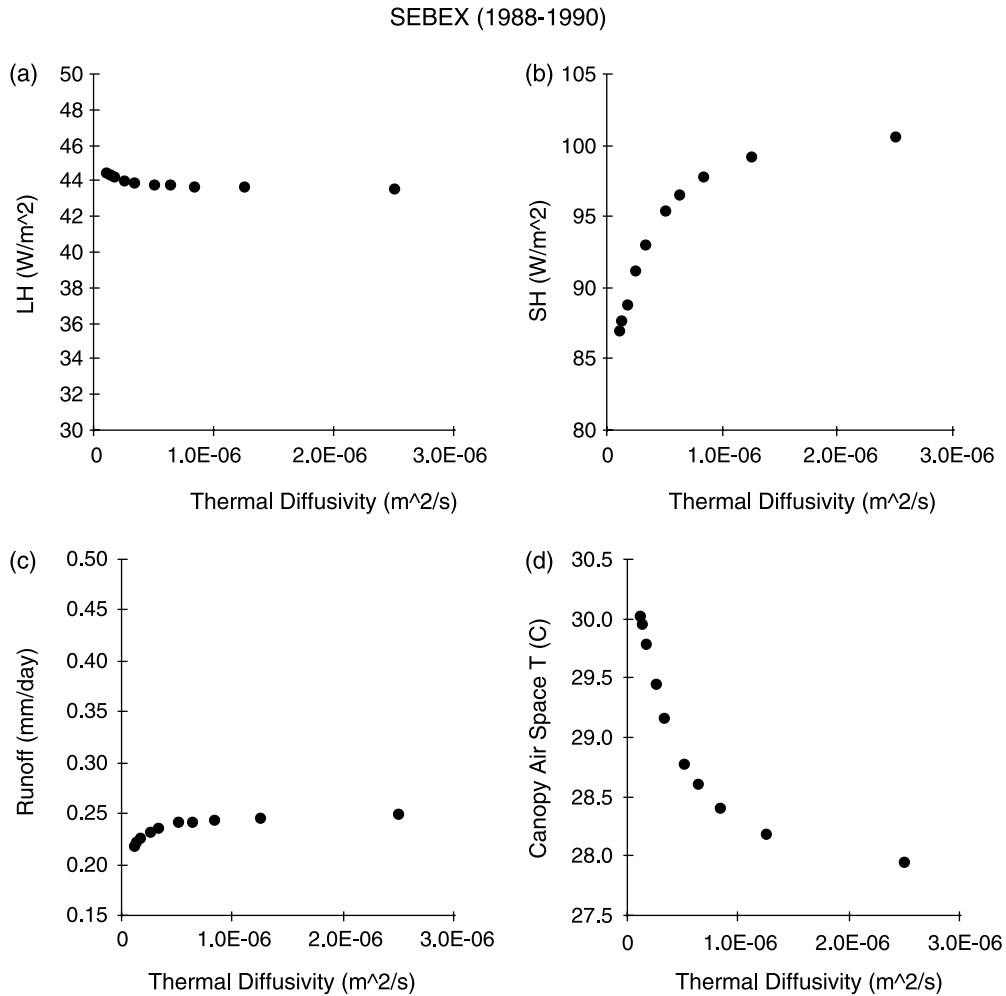


Fig. 12. Average (a) latent heat flux (W m^{-2}), (b) sensible heat flux (W m^{-2}), (c) runoff (mm day^{-1}), and (d) canopy air space temperature ($^{\circ}\text{C}$) over 2-year SEBEX period, varying by thermal diffusivity ($\text{m}^2 \text{s}^{-1}$).

error is reduced from 48.2 to 29.6 W m^{-2} , much closer to the observational RMS error of 24.7 W m^{-2} . Furthermore, the correlation coefficient, based on daily data, improves from 0.76 to 0.89 .

At the same time, the simulation of sensible heat flux (Figs. 6b and 7b) is significantly improved. The correlation coefficient, which was 0.51 for S-1, improves to 0.80 for daily data. In addition, the diurnal cycle of the sensible heat flux is accurately simulated (Fig. 7b). Run S-2 leads to an average of 53.5 W m^{-2} , very close to the observation of 57.8 W m^{-2} . The RMS error is reduced from 30.6

to 18.2 W m^{-2} . This accurate simulation indicates that the simulation's differences from observations in the latent heat flux might be mainly due to the observational error. The improper partitioning between latent heat and ground heat flux might also contribute to the differences.

The RMS error of ground heat flux (Figs. 6c and 7c) in S-2 increased slightly, from 8.56 to 9.55 W m^{-2} . This slight deterioration is consistent with the simulation in surface canopy temperature. The average ground heat flux increased very slightly from 1.2 to 2.2 W m^{-2} .

There was only a minor change in the average surface temperature (Figs. 6d and 7d), with the results from S-1 and S-2 being 30.9 and 31.2 °C, respectively, as compared with 29.9 °C observed. Similar to H-2, the RMS error increased only slightly from 1.39 to 1.50 °C. The new thermal diffusivity, as expected, reduced surface temperature during the daytime and increased it at nighttime (Fig. 7d). Since S-1 already produced proper surface temperature, the new data set slightly deteriorated the simulation for surface temperature and ground heat flux in S-2.

The friction velocity showed no significant change in the average or the RMS error. The soil wetness as compared with observations showed little difference at the top layer. In the second layer (Fig. 8), however, the new data set improved the average from 0.37 to 0.24, closer to the observed average of 0.18.

7. Conclusion

A series of numerical experiments was designed to understand the physics at the soil/vegetation–atmosphere interface, to find the major parameterizations/parameters that are crucial for simulating arid climate processes, and to examine how parameter calibration would improve model simulation. Two observational data sets, HAPEX-Sahel and SEBEX, were used to help interpret the results. Their errors were discussed first to provide a reference for model evaluation.

The study shows that LAI, stomatal resistance, and hydraulic conductivity at saturation are important to simulate latent heat flux and sensible heat flux, especially during the daylight hours. With more available observed surface fluxes and surface variables, such as soil moisture and surface temperature, than previous studies such as Xue et al. (1996), this study further explores the role of surface parameters in the Sahel region. It is found that soil properties, including thermal diffusivity, play an important role in the surface water and energy budgets. Usually, standard GCM vegetation values vary by the month, but such an infrequent change in this parameter may not be enough to accurately reflect the change in plant composition that occurs as a reaction to climatic conditions. The simulation's sensitivity to the timing of LAI shows that higher temporal resolution of this

surface parameter may be necessary for proper simulation of seasonal variation of evaporation. Type-8 LAI was still used for the SEBEX data set from November through July, which may explain some of the error in the SEBEX validation run.

The decrease of stomatal resistance and the increase of hydraulic conductivity, each by more than one order of magnitude, also serve to increase evaporation in runs H-2 and S-2. The changes in the data set are consistent throughout the year but have the greatest effect during wet months. Fig. 6a, for example, shows little difference in latent heat flux between runs S-1 and S-2 during the dry months, but during the wet months the difference is evident. In particular, proper parameter values during wet conditions may play an important role.

In this study, we first identify the key parameters and then adjust them based on the relationship discovered in sensitivity studies and the errors in control runs. Because of the clear physical implications in this process, just a few trial and error tests are required in this study with only a single site. In general, the calibrated set of vegetation parameters produced a significantly different energy balance from the standard parameters. The increase in LAI and reduction in stomatal resistance allowed for more transport of moisture from the land surface to the atmosphere. This change in latent heat flux also served to reduce sensible heat flux, bringing them both much closer to observations, with significantly reduced RMS errors. On a diurnal scale, the greatest difference between the control and experimental runs exists during the day; on a monthly scale, there appears to be the greatest difference during the wet months. Although the deviation of ground heat flux from the observations increased, it remained less than the observational error. Because the observational data are also subject to significant error, any discussions about model errors should take into account these errors. Water balance components are also more consistent with observations when the calibrated parameter set is implemented. Evaporation and runoff are both increased, reducing the overestimation of soil moisture content found in both control runs.

This study demonstrates that although standard vegetation parameters may work well in GCMs, they can be subject to many possible flaws. Xue et al. (1997), based upon a number of off-line tests,

indicated that, for simulation at a single site, proper parameter values are crucial and use of parameters from the GCM vegetation data set may lead to substantial errors. Furthermore, the standard values for the presumed land cover type are an average of many similar types of vegetation; they cannot account for the natural variability within the vegetation class (Los et al., 1994). They may not account for recent growth or senescence of the vegetation either. For these reasons, other sources of data such as satellite data may be preferable when available.

Solar radiation and precipitation are driving factors in any environment, but the sensitive nature of arid climates makes the reaction of the land surface to climate especially important. Better parameterization of surface conditions in these areas should help improve the reliability of GCM experiments, which are vital in the simulation of climate in threatened regions such as the Sahel. This study only employed SSiB. The results and the final parameter set are model dependent. Multi-model experiments undertaken by MOPEX would be very helpful to understand the uncertainty in deriving model parameter values and understanding the mechanisms of land/atmosphere interactions. A number of methods have been developed to best estimate parameters of land surface models (Gupta et al., 1999; Duan et al., 2001; Jackson et al., 2003). Workshops for parameter estimation such as MOPEX will serve to improve regional model applications in many different areas by promoting the transfer of parameter estimation knowledge between different modeling groups (Duan et al., 2005).

Acknowledgements

The authors thank the Center for Ecology and Hydrology, United Kingdom, for providing the HAPEX-Sahel and SEBEX data. Funding was provided by NSF ATM-0097260.

References

- Allen, S.J., Wallace, J.S., Gash, J.H.C., Sivakumar, M.V.K., 1994. Measurements of albedo variation over natural vegetation in the Sahel. *Int. J. Climatol.* 14, 625–636.
- Bastidas, L.A., Gupta, H.V., Sorooshian, S., Shuttleworth, W.J., Yang, Z.L., 1999. Sensitivity analysis of a land surface scheme using multi-criteria methods. *J. Geophys. Res.* 104 (D16), 19481–19490.
- Blyth, E.M., 1997. Representing heterogeneity at the southern super site with average surface parameters. *J. Hydrol.* 188–189, 869–877.
- Charney, J.G., 1975. Dynamics of deserts and drought in the Sahel. *Q. J. R. Meteorol. Soc.* 101, 193–202.
- Dickinson, R.E., Henderson-Sellers, A., 1988. Modeling tropical deforestation: a study of GCM land-surface parameterizations. *Q. J. R. Meteorol. Soc.* 114, 439–462.
- Dickinson, R.E., et al. 1986: Biosphere-atmosphere transfer scheme (BATS) for the NCAR community climate model. NCAR/TN - 275 + STR.
- Dolman, A.J., Gregory, D., 1992. The parameterization of rainfall interception in GCMs. *Q. J. R. Meteorol. Soc.* 118, 455–467.
- Dolman, A.J., Allen, S.J., Lean, J., 1993. Climate simulations of the Sahel: a comparison with surface energy balance observations, exchange processes at the land surface for a range of space and time scales. *Proc. Yokohama Symp. IAHS* 212, 513–519.
- Dolman, A.J., Culf, A.D., Bessemoulin, P., 1995. Observations of boundary layer development during the hapex-sahel intensive observation period. *J. Hydrol.* 188–189, 998–1016.
- Dorman, J.L., Sellers, P., 1989. A global climatology of albedo, roughness length and stomatal resistance for atmospheric general circulation models as represented by the Simple Biosphere Model (SiB). *J. Appl. Meteorol.* 28, 833–855.
- Duan, Q., Schaake, J., Koren, V., 2001. A priori estimation of land surface model parameters. In: Lakshmi, V. et al. (Ed.), *Land Surface Hydrology, Meteorology, and Climate: Observations and Modeling Water Science and Application*, vol. 3. American Geophysical Union, Washington, DC, pp. 77–94.
- Duan, Q., Schaake, J., Andreassian, V., Franks, S., Gupta, H.V., Gusev, Y.M., Habets, F., Hall, A., Hay, L., Hogue, T., Huang, M., Leavesley, G., Liang, X., Nasonova, O.N., Noilhan, J., Oudin, L., Sorooshian, S., Wagener, T., Wood, E.F., 2005. Model parameter estimation experiment (MOPEX): overview and summary of the second and third workshop results. *J. Hydrol.* x-ref: DOI 10.1016/j.jhydrol.2005.07.03.
- Gash, J.H.C., et al., 1991. Measurements of evaporation from fallow Sahelian savannah at the start of the dry season. *Q. J. R. Meteorol. Soc.* 117, 749–760.
- Goutorbe, J.P., et al., 1994. HAPEX-Sahel—A large-scale study of land-atmosphere interactions in the semi-arid tropics. *Ann. Geophys.* 12, 53–64.
- Goutorbe, J.P., et al., 1997. An overview of HAPEX-Sahel: a study in climate and desertification. *J. Hydrol.* 188–189, 4–17.
- Gupta, H.V., Bastidas, L.A., Sorooshian, S., Shuttleworth, W.J., Yang, Z.L., 1999. Parameter estimation of a land surface scheme using multi-criteria methods. *J. Geophys. Res.* 104 (D16), 19491–19504.
- Hanan, N.P., Prince, S.D., 1997. Stomatal conductance of west-central supersite vegetation in HAPEX-Sahel: measurements and empirical models. *J. Hydrol.* 188–189, 536–562.

- Hogue, Terri, 2004. Model parameter experiment begins new phase. *EOS* 85, 217–218.
- Jackson, C., Xia, Y., Sen, M., Stoffa, P., 2003. Optimal parameter and uncertainty estimation of a land surface model: a case example using data from Cabauw, Netherlands. *J. Geophys. Res.* 108, 4583. doi:10.1029/2002JD002991.
- Kitoh, A., Yamazaki, K., Tokioka, T., 1988. Influence of soil moisture on surface albedo changes over the African tropical rain forest on summer climate investigated with the MRI-GCM-I. *J. Meteorol. Soc. Jpn* 66, 65–85.
- Laval, K., Picon, L., 1986. Effect of a change of the surface albedo of the Sahel on climate. *J. Atmos. Sci.* 43, 2418–2429.
- Liu, Y., Gupta, H.V., Sorooshian, S., Bastidas, L.A., Shuttleworth, W.J., 2004. Exploring parameter sensitivities of the land surface using a locally coupled land-atmosphere model. *J. Geophys. Res.* 109, D21101. doi:10.1029/2004JD0047.
- Los, S.O., Justice, C.O., Tucker, C.J., 1994. A global 1 by 1 degree NDVI data set for climate studies derived from the GIMMS continental NDVI data. *Int. J. Remote Sensing* 15, 3493–3518.
- Sellers, P.J., Mintz, Y., Sud, Y.C., Dalcher, A., 1986. A simple biosphere model (SiB) for use with general circulation models. *J. Atmos. Sci.* 43, 505–530.
- Sud, Y.C., Fennessy, M., 1982. A study of the influence of surface albedo on July circulation in semiarid regions using the GLAS GCM. *J. Climatol.* 2, 105–125.
- Taylor, C.M., Blythe, E.M., 2000. Rainfall controls on evaporation at the regional scale: an example from the Sahel. *J. Geophys. Res.* 105, 15469–15479.
- Taylor, C.M., Saïd, F., Lebel, T., 1997. Interactions between the land surface and mesoscale rainfall variability during HAPEX-Sahel. *Mon. Wea. Rev.* 125, 2211–2227.
- Walker, J., Rowntree, P.R., 1977. The effect of soil moisture on circulation and rainfall in a tropical model. *Q. J. R. Meteorol. Soc.* 103, 29–46.
- Wallace, J.S., et al., 1991. The Sahelian energy balance experiment (SEBEX): ground based measurements and their potential for spatial extrapolation using satellite data. *Adv. Space Res.* 11 (3), 131–141.
- Xue, Y., 1997. Biosphere feedback on regional climate in tropical North Africa. *Q. J. R. Meteorol. Soc.* 123, 1483–1515.
- Xue, Y., Shukla, J., 1993. The influence of land surface properties on Sahel climate. part I: desertification. *J. Climate* 6, 2232–2245.
- Xue, Y., Sellers, P.J., Kinter III, J.L., Shukla, J., et al., 1991. A simplified biosphere model for global climate studies. *J. Climate* 4, 345–364.
- Xue, Y., Bastable, H.G., Dirmeyer, P.A., Sellers, P.J., 1996a. Sensitivity of simulated surface fluxes to changes in land surface parameterizations—a study using ABRACOS data. *J. Appl. Meteor.* 35, 386–399.
- Xue, Y., Zeng, F.J., Adam, C., 1996b. SSiB and its sensitivity to soil properties—a case study using HAPEX-Mobilhy data. *Global Planet. Change* 13, 183–194.
- Xue, Y., Sellers, P.J., Zeng, F.J., Schlosser, C.A., 1997. Comments on ‘Use of midlatitude soil moisture and meteorological observations to validate soil moisture simulations with biosphere and bucket models’. *J. Climate* 10, 374–376.